DEVELOPING A FRAMEWORK FOR MODELING TRANSMISSION THROUGH INHOMOGENOUS GERMANIUM ANTIMONY TELLURIDE (GST) THIN FILMS

Benjamin Belfore and Sylvain Marsillac
[1] Virginia Institute of Photovoltaics, Old Dominion University, Norfolk, VA, USA

***Abstract* — Infrared Spectral Imaging is a powerful tool for both atmospheric sciences and astronomy. When trying to determine the composition of Earth's atmosphere or other planets, a significant amount of information can be gleaned by observing the mid-wave infrared (MWIR) spectrum. While there are various ways to observe this range of the spectrum, there has recently been a push to implement filters in this region that are more precisely tunable to decrease the Size, Weight, and Power (SWAP) burden for satellites. One material that has shown promise is Germanium Antimony Telluride or GST. By annealing the GST at different temperatures, its crystalline structure and optical properties both change. By exploiting this phenomena, it is possible to create a narrowband filter in the MWIR spectrum. Since the properties are changed, typically through heating via laser pulses, it is possible that localized inhomogeneities could remain post annealing. Using phase field simulations for recrystallization and both ray tracing and transfer matrix method, the impact of these potential inhomogeneities are explored.**

I. Introduction

The mid-wave infrared (MWIR) spectrum is particularly important to atmospheric sciences because it can be used to detect various chemicals in the air. This is because the wavelengths in the MWIR band (3-5 μm) coincide with the resonant frequencies of the chemical bonds within atoms.[1] This absorption results in a significant increase in absorption of infrared right at specific, known wavelengths. In a laboratory setting, this phenomenon can be exploited in powerful characterization techniques like Fourier transform infrared spectroscopy (FTIR).[2] When applied to atmospheric sciences or astronomy, these techniques can be used to find the composition of both our planets and other celestial body's atmospheres.[1,3]

While MWIR spectral imaging has already been implemented in satellites, current technologies have some significant limitations. One of the key ways that space-based technology is evaluated is by examining its Size Weight and Power (SWAP). By minimizing the SWAP cost it is possible to both lower the cost of a satellite and fit additional instrumentation on said satellite.

To perform MWIR spectral imaging, a filter assembly is needed. This is because certain chemical species have certain vibrational modes that need to be characterized. For example, of particular interest to environmental scientists is the 4.5 μm wavelength, which is one of the primary vibrational modes of CO_2.[4] The current technology used in MWIR filters is similar to technology used in filters in the visible spectrum. To accommodate to the shift to the MWIR spectrum, new materials and narrower band gap semiconductors were necessary; because the applications of these semiconductors are narrower, less work has been done on them. This has significantly increased the cost of traditional-style MWIR filters.[5] Also, many of these MWIR filters have a moving component like a filter wheel.[6] While not directly related to SWAP, minimizing the amount of moving parts in an instrument being sent to space decreases the possibility of the piece of equipment failing.

For all of the reasons discussed above, developing a new type of MWIR filter that would be ideal for space implementation would be ideal. Ideally this new filter would have minimal moving parts, have a tunable wavelength to probe various vibrational modes of interest, and have a low SWAP burden. These goals align well with adaptive optics. One material that shows a significant degree of promise in the adaptive optics world is Germanium Antimony Telluride (GeSbTe) or GST. GST has been used since the 80s in rewritable CDs and has found newer applications in phase change random access memory. By annealing GST at various temperatures, the crystalline structure can change from amorphous to Face-Centered Cubic (FCC) to Hexagonal Closed Pack (HCP). Depending on the crystalline phase of GST, both its electrical and optical properties vary significantly.[7] By implementing GST in tunable optics, it could be possible to further decrease the SWAP burden of MWIR spectral imaging on satellites.

While GST shows promise, there are some limitations. Currently, one of the most common techniques for changing the phase of GST is heating via pulsed laser. While this technique works in most cases, over repeated heating and cooling cycles inhomogeneities could occur due to partial crystallization. While there has been some experimental work examining the partial crystallization of GST, to our knowledge, there has not been a rigorous simulation approach to examine the impact of partial crystallization on optical properties.[8]

II. Simulation Methodology and results

To model transmission through partially crystallized GST, two different types of simulations were necessary. The first portion was to simulate a recrystallization process within GST. While many different techniques can be used to model

crystallization, phase field was used because it creates a continuous domain, and it is equation driven as opposed to statistically driven. This will allow for further refinement and parameterization down the line. After the crystallization simulations were completed, optical simulations needed to be performed. One of the most common optical simulation techniques used is the transfer matrix method. While it is a powerful technique for optical simulations, it is only viable in stratified media. Since the result of the crystallization simulations will be random and non-stratified, it is not viable as is. To circumvent that issue, ray tracing was performed to find the optical path of the light moving through the film. With a known optical path through the media, the result of the ray tracing model can be reduced to a 1-dimensional model and the transfer matrix method could then be used.

A. Phase Field

While there are multiple ways to model recrystallization, phase field allows significantly more latitude with parameterization. In a phase field simulation, the different domains are defined by an order parameters: η_i. where i is the number of field variables. In phase field simulations, the order parameters are continuous, non-conserved, and vary from 1 (within the domain) to 0 (outside of the domain). The crystallization process is governed by the time-dependent Gisnburg Landau equation in the following form:[9]

$$\frac{\partial \eta_i(r,t)}{\partial t} = -L_i \frac{\delta F}{\delta \eta_i(r,t)} \quad i = 1,2,\dots,n \qquad (1)$$

Where η_i is the field variable, L_i is a relaxation coefficient, r is related to the spatial dimension of the field, and F is the microstructure grain boundary energy in the system with:

$$F = \int_V f(\eta_1,\dots,\eta_n) + \sum_{i=1}^{n} \frac{\kappa_i}{2} (\nabla \eta_i)^2 \, dV \qquad (2)$$

Where κ is the gradient of free energy density and f is the local free energy density which can be defined as:[10]

$$f(\eta_1,\dots,\eta_n) = \sum_{i=1}^{n} \left(-\frac{\alpha}{2}(\eta_i)^2 + \frac{\beta}{4}(\eta_i)^4 \right) + \gamma \sum_{i=1}^{n} \sum_{j \neq i}^{n} \eta_i^2 \eta_j^2 \qquad (3)$$

Where α, β, and γ are phenomenological constants.[9] For our simulations all 3 constants were set to 1 and κ_i was set to 1 as well. These equations were solved within COMSOL Multiphysics on a high-performance cluster. Because of the nonlinearity of the system of partial differential equations, simulation times were significant and, while multiple phases up to 36 were tested, 4 were used to increase the number of simulations that could be performed.

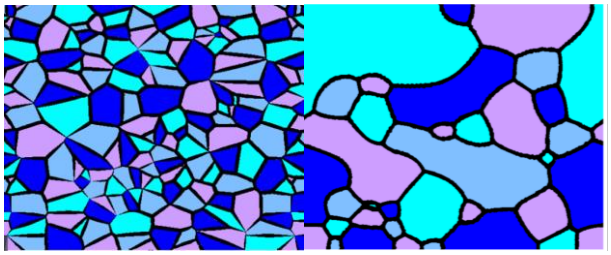

Figure 1: Phase field simulation at t=0 (left) and t= 1000 (right).

As figure 1 shows, phase field is an excellent technique for modelling microstructure evolution, but there are some severe limitations. Common to many techniques used to model recrystallization, the simulated time is not directly analogous to an actual time. The other key limitation is the lack of direct relation to the spatial dimension. While the simulation does have a discrete domain, it is not feasible to relate that size of the domain to a direct, quantifiable value. For the subsequent optical simulations, 1 pixel was assumed to be 1 nm.

B. Ray Tracing

Phase field simulations create a significant amount of raw data, and post processing on the data directly is computationally intensive. To minimize the amount of preprocessing on the optical simulation end, the simulation results were taken as a high-resolution image from COMSOL and imported into MATLAB. Each discrete phase was then separated from the others using image processing to create a mask of each. This separation provides two distinct advantages. Since each phase is separated from the other defining the areas of different refractive indices is trivial. Also since four masks were necessary, the grain boundaries derived from these masks is a composite of all four masks, decreasing optical errors in the grain boundary structure.

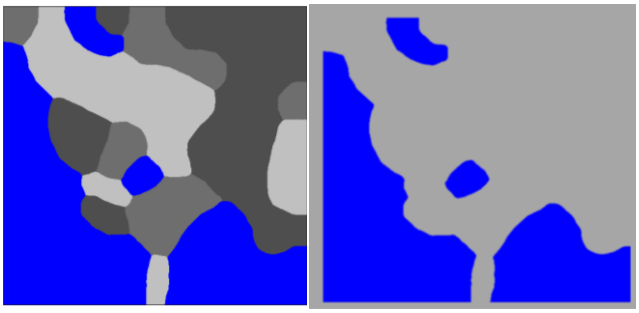

Figure 2 Output image from COMSOL (left). Mask of only one phase (right).

The images were then binarized and the edge pixel between the mask and the outlying areas was found. Thereafter, a composite grain structure was generated using the binary images of the 4 masks (Figure 3).

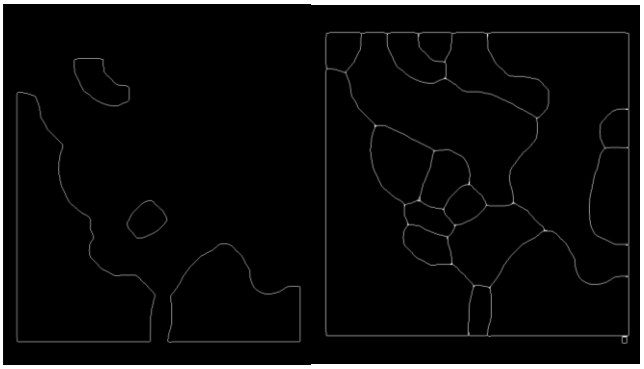

Figure 3: a single grain boundary structure from one phase (left) the combination of all 4 structures (right).

By using the masks to define refractive index and the binary grain structure to define interfaces, it is possible to do some initial ray tracing simulations.

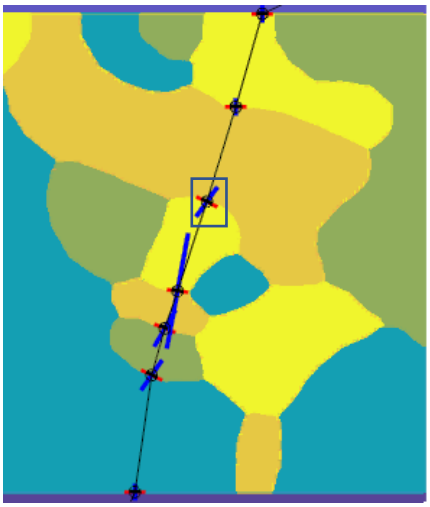

Figure 4: Example of light ray raveling through a completed phase field simulation with the tangent line to the interface (red) and normal (blue) shown. The square shows the location of interest for figure 5.

As figure 4 shows, we can successfully perform a ray trace through the layer. To do this effectively, two things need to be done: accurate interface tracing and proper implementation of Snell's law.

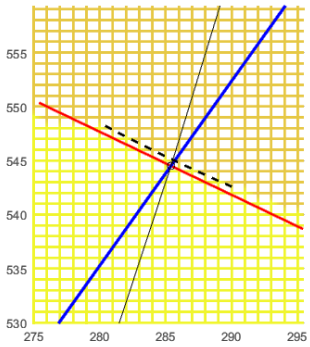

Figure 5: the interface of interest in figure 4.

To find the interface, the ray travels through a field similar to figure 3. This is done by using a bilinear operator to interpolate between pixels, and, when a grain boundary is detected, a number of pixels are traced on each side. Using those pixels, a 2-degree polynomial is fit. The tangent is then found by calculating the derivative of the polynomial at the point of intersection and the normal is taken as the negative reciprocal of that slope.

One of the key problems with performing an optical simulation on layers like this is the fact that the media through which the light is moving is non-stratified, meaning they are not well defined layers. Because of this, the location of the interface and the angle with respect to the incident light is not known. To find this, a modified Snell's law was used:

$$n_1 \sin(\theta_{ri}) = n_2 \sin(\theta_{rt}) \qquad 4$$

Where n is the refractive index and θ_{ri} and θ_{tr} are the relative angle of incidence and transmission respectively. θ_{ri} is the angle between the angle of the traveling ray and the surface normal vector given by

$$\cos(\theta_{ri}) = \frac{\overrightarrow{v_{light}} \cdot \overrightarrow{v_{normal}}}{\left\|\overrightarrow{v_{light}}\right\| \left\|\overrightarrow{v_{normal}}\right\|} \qquad 5$$

To account for the multiple directions the ray could be traveling, θ_{ri} was calculated for both directions of $\overrightarrow{v_{normal}}$ with the smallest value being taken. A similar methodology is then utilized to ensure that the ray continues in the appropriate direction.

As figures 3 and 4 show, this methodology for ray tracing works well for transmission, while only total internal reflection is implemented in the model. Dependence on the refractive index needs to be implemented to make this system viable for a

transfer matrix method process. To make these simulations more relevant for MWIR applications, it is necessary to make the refractive index vary with the wavelength.

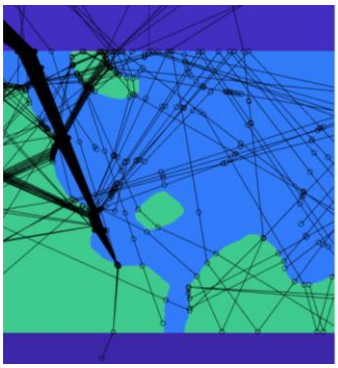

Figure 6: Ray tracing process with refractive index varying with λ

Figure 6 collapses the previously shown system into two regions. Region 1, the teal region, has the refractive index of HCP GST, and the light blue has the refractive index of amorphous GST. The wavelengths used varied from 1 to 10 μm. The refractive index of the HCP region varies between 5.2 and 6.3; the refractive index of the amorphous region varies between 2.9 and 3.4.[6]

C. Transfer Matrix Method

The previously shown ray tracing process indicates qualitatively how inhomogeneities could be problematic to the optical path through the GST film. To expand on this, a modified transfer matrix method was used to determine the transmission through the film. This was done by calculating the optical path of rays that fully travelled through the film. Using this optical path distance, it is possible to convert the 2-dimensional simulation into a one dimensional structure. With this reduction in dimensionality, transfer matrix method becomes viable.

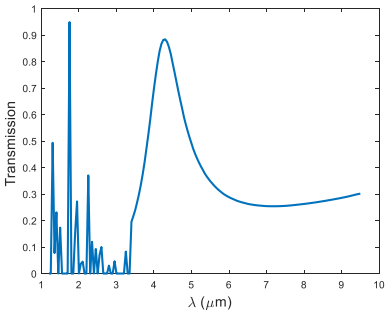

Figure 7: The transmission curve obtained by the ray trace in figure 6

The transmission obtained in figure 7 aligns well with the resulting ray tracing seen in figure 6. In the near IR spectrum and early Middle IR spectrum, a significant amount of transmission is blocked due to the large difference in refractive index between the amorphous and HCP crystalline structure. While this large degree of separation is beneficial for creating band pass filters, these inhomogeneities can be severely detrimental.

To reinforce the validity of the simulations, another simulation with slight differences in refractive index can be examined. While the difference in the HCP and amorphous refractive index is significant, the difference between the HCP and FCC is not as much.

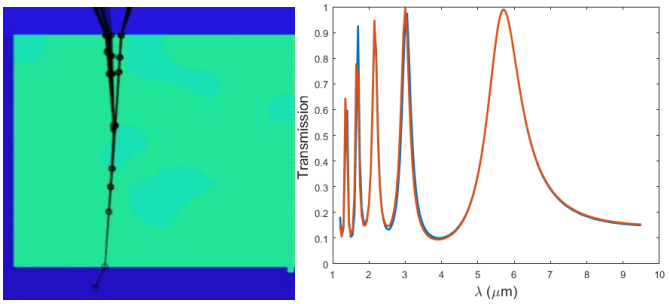

Figure 8: Gentle refraction with inhomogeneity with close refractive index (left). Comparing the slight refraction with a homogenous layer with homogenous (blue) and non-homogeneous (orange) transmission

As figure 8 shows, even a minor inhomogeneity can change the path that the ray can travel. While it only has a modest impact on the transmission, when one considers the more common amorphous to HCP transmission, the inhomogeneities become much more impactful (Figure 9).

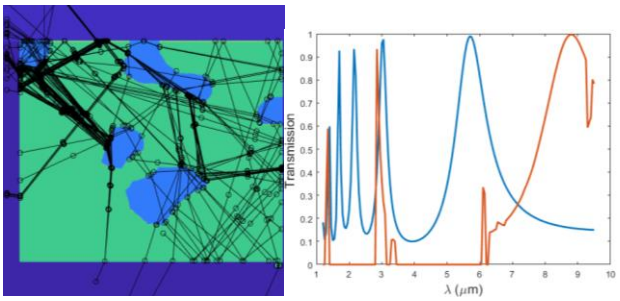

Figure 9: Example of a low refractive index material imbedded in a high refractive index material (Amorphous in HCP)

Obviously, there is significantly more scattering when the difference in refractive index becomes higher. Examining the HCP to a phase change is also more important because it is more relevant for the application of narrow MWIR band filters.

III. Conclusion

Combining phase field simulations with optical simulations is an innovative approach to analyzing the impact of inhomogeneities in optical properties. Moving forward, additional simulation refinement could be performed to further improve the parameterization of the phase field equations. Additional parallelization could also be implemented in order to account for transmission and reflections at both interfaces, but, as the TMM approach shows, current simulation results are still valid.

Acknowledgement

This research was funded via a graduate research fellowship through the Virginia Space Grant Consortium

References

[1] G. J. Hawkins, R. E. Sherwood, B. M. Barrett, M. Wallace, H. J. B. Orr, K. Matthews, and S. Bisht, "High-performance infrared narrow-bandpass filters for the Indian National Satellite System meteorological instrument (INSAT-3D)," Appl. Opt. 47, 2346-2356 (2008).

[2] M.E. Pemble and P. Gardner, "Vibration spectroscopy from surfaces," in *Surface Analysis: The Principle Techniques*, 2nd ed. J. C. Vickerman and I. S. Gilmore, Ed. Western Sussex, U.K.: A. John Wiley and sons ltd, 2009, pp-333-386.

[3] G. Shaw and H. Burke, "Spectral imaging for remote sensing", *Lincoln Lab. J.*, vol. 14, no. 1, pp. 3-28, 2003.

[4] Calum Williams, Nina Hong, Matthew Julian, Stephen Borg, and Hyun Jung Kim, "Tunable mid-wave infrared Fabry-Perot bandpass filters using phase-change GeSbTe," Opt. Express 28, 10583-10594 (2020).

[5] A. Rogolaski. "Infrered detectors: an overview," *Infrared Physics and Technology*, vol. 43, no. 3-5, pp. 187-210, 2002.

[6] Matthew N. Julian, Calum Williams, Stephen Borg, Scott Bartram, and Hyun Jung Kim, "Reversible optical tuning of GeSbTe phase-change metasurface spectral filters for mid-wave infrared imaging," Optica 7, 746-754 (2020).

[7] P. Guo, A. M. Sarangan, and I. Agha, "A review of germanium-antimony-telluride phase change materials for non-volatile memories and optical modulation," *Applied Sciences*, vol. 9, no. 3, pp. 530, February 2019.

[8] H. -S. P. Wong *et al*., "Phase Change Memory," in *Proceedings of the IEEE*, vol. 98, no. 12, pp. 2201-2227, Dec. 2010.

[9] M.A. Zaeem, H.E. Kadiri, P. Wang, M. Horstemeyer "Investigating the effects of grain boundary energy anisotropy and second-phase particles on grain growth using a phase-field model" Comput. Mater. Sci. 50 ,pp. 2488-2492, (2011).

[10] N. Moelans, B. Blanpain, and P. Wollants,, "Phase field simulations of grain growth in two-dimensional systems containing finely dispersed second-phase particles" Acta Materialia, Volume 54, Issue 4,, pp. 1175-1184, 2006.